SCIENTIFIC ARTICLE

Distribution of Nerve Endings in Human Distal Interphalangeal Joint and Surrounding Structures

Takako Chikenji, MPH, Richard A. Berger, MD, PhD, Mineko Fujimiya, MD, PhD, Daisuke Suzuki, PhD, Sadako Tsubota, Kai-Nan An, PhD

Purpose To examine the distribution of encapsulated nerve endings called mechanoreceptors in the human distal interphalangeal (DIP) joint and surrounding structures.

Methods We processed 12 right index finger DIP joints and surrounding structures from fresh cadavers for immunohistochemistry of the anti-protein gene product 9.5 (PGP9.5) and silver staining to detect encapsulated nerve endings. Serial transverse sections were cut throughout the whole specimen and divided into 3 regions along the longitudinal axis: distal, middle, and proximal. Each of the transverse sections was partitioned into dorsal capsule (DC), radial capsule (RC), ulnar capsule (UC), volar plate (VP), and radial and ulnar assemblage nuclei (RAN and UAN); the RAN and UAN are located on both the radial and ulnar side of the VP. The C3 pulley contained the proximal region of the RAN and UAN, whereas the A5 pulley contained the middle and distal. The accessory collateral ligament contained all the regions of the RAN and UAN. We analyzed and compared the density of encapsulated nerve endings among the 18 different regions.

Results According to the modified Freeman and Wyke classification, we identified type I (eg, Ruffini-like endings) and type II (eg, Pacini-like endings) nerve endings. The density of type II nerve endings in the proximal region of the RAN and UAN was considerably higher than that in the proximal region of the VP, RC, UC and DC, and that in the proximal region of the VP, RC, UC, and DC, respectively.

Conclusions Our examination of the distribution of type I and type II nerve endings provides new information on the sensory systems of the DIP joints and surrounding structures. *(J Hand Surg 2011;36A:406–412. Copyright © 2011 by the American Society for Surgery of the Hand. All rights reserved.)*

Key words Immunohistochemistry, mechanoreceptor, nerve ending, distal interphalangeal joint, pulley system.

THE HUMAN FINGER performs its fine manipulative activities through a well-integrated sensory-motor system. Sensory feedback from the finger has a role in the control of its manipulative and exploratory movements. Encapsulated nerve endings called mechanoreceptors are end components of afferent inflows and have specialized end organs surrounding the nerve terminal.[1] Those receptors are enriched in various human periarticular tissues[2–4] and have been classified into 3 types[5]: type I (Ruffini-like ending), type II (Pacini-like ending), and type III nerve endings (Golgi-like tendon organ). All mechanoreceptors react to mechanical stimuli and each nerve ending has individual physiological characteristics.[1,6,7] It has been postulated that type I nerve endings respond to stretch stimuli,[1,7] type II endings to pressure and vibratory stimuli,[1] and type III endings to considerable stress at the extremes of their range of movement.[6] However, it is not

From the Orthopedic Biomechanics Laboratory, Division of Orthopedic Research, Mayo Clinic, Rochester, MN; and the Graduate School of Health Science and the Department of Anatomy, Sapporo Medical University, Sapporo, Hokkaido, Japan.

Received for publication October 14, 2010; accepted in revised form November 29, 2010.

The authors thank Drs. T. Kamiya, H. Chiba, and M. Aoki for skillful help with staining, and M. Umeda for cadaver management.

Corresponding author: Richard A. Berger, MD, PhD, Mayo Clinic, Orthopedic Biomechanics Laboratory, 200 First Street SW, Rochester, MN 55905; e-mail: berger.richard@mayo.edu.

0363-5023/11/36A03-0005$36.00/0
doi:10.1016/j.jhsa.2010.11.050

known which type of mechanoreceptors in periarticular tissues contribute to proprioceptive sensibility[8,9] and to modulation of protective muscle responses.[10–12]

In our previous studies, encapsulated nerve endings in the human proximal interphalangeal (PIP) joint and surrounding structures were extensively examined.[13] We identified type I and type II nerve endings in the PIP joint and surrounding structures. Although the type I nerve endings were notably distributed in the proximal volar plate in the PIP joint and surrounding structures, the type II nerve ending was substantially distributed in both the proximal radial and ulnar assemblage nuclei (RAN and UAN). The proximal RAN and UAN in the PIP joint and surrounding structures are located on both the radial and ulnar sides of the volar plate and contained the C1 pulley and accessory collateral ligaments. The distribution of type I and II nerve endings suggests that the C1 pulley, accessory collateral ligament, and volar plate might relate to sensory function of the finger.

In the human finger joint and surrounding structures, the distal interphalangeal (DIP) and PIP joints have a similar anatomy and pulley system.[14–17] The DIP and PIP joints and surrounding structures are composed of volar plate, collateral ligament, accessory collateral ligament, flexor and extensor tendon, and pulley. The cruciate pulley is located distal to the annular pulley in both DIP and PIP joints: The C1 pulley is located distally to the A2 pulley in the PIP joint, whereas the C3 pulley is located distal to the A4 pulley in the DIP joint.[14] In addition, both the C1 and C3 pulleys have 1 fixed attachment to bone and 1 moveable attachment to the volar plate.[14]

In the human pulley system, the functional importance of the annular pulley has been well established[14,15,18]; however, it is believed that the cruciate pulley is unlikely to serve a major mechanical function.[15] Our objective was to quantitatively analyze the distribution of the encapsulated nerve endings in the human DIP joint and surrounding structures, to better understand the new function of the cruciate pulley and the well-integrated sensory-motor systems in the fingers.

MATERIALS AND METHODS

We obtained 12 DIP joints and surrounding structures of the right index fingers (10 men and 2 women) from fresh-frozen cadavers. The mean age at the death for the subjects was 85 years (range, 73–96 y). We found no apparent injury or deformation of fingers. The skin was removed and the specimens included the DIP joint and surrounding structures between the origin and the insertion of both collateral ligaments (length, 10–12 mm). We did not include the flexor digitorum profundus tendon because the tendon was located over the volar plate throughout the DIP joint, and the tendon did not contact the actual joint. We defined the DIP joint as the area between the origin and the insertion of both collateral ligaments. Therefore, the flexor digitorum profundus tendon did not lie within the DIP joint as we have defined it. However, we included the extensor tendon because the extensor tendon contacted the actual joint.

Serial transverse sections were cut throughout the whole specimen. Transverse sections were extracted at 500-μm intervals and stained by immunohistochemistry and silver staining to detect 3 types of nerve ending.[5]

Type I nerve ending (Ruffini-like ending)

The shape is globular or oval. The thin capsule encloses fine arborizing nerve filaments. The average size is 100 × 40 μm. The physiological characteristics are low threshold, slowly adapting.

Type II nerve ending (Pacini-like ending)

The shape is cylindrical or conical. A single-axis cylinder is surrounded by a laminated capsule. The average size is 280 × 120 μm. The physiological characteristics are low threshold, rapidly adapting.

Type III nerve ending (Golgi-like ending)

The shape is fusiform. The thin capsule surrounds coarse, arborizing nerve filaments. The average size is 600 × 100 μm. The physiological characteristics are low threshold, very slowly adapting.

We used immunohistochemical staining to detect type I and type III nerve endings.[5] Type I nerve endings were differentiated from type III nerve endings by their size. We used hematoxylin-eosin staining to show the morphology of the DIP joint and surrounding structures.

We used silver staining to detect type II nerve endings, the morphological features of which are thick lamella formations.[5]

Immunohistochemical procedure (type I and type III nerve endings)

We immersed 6 DIP joints for 24 hours in 4% paraformaldehyde, 0.5% glutaraldehyde, and 0.2% picric acid in 0.1 mol/L phosphate buffer (PB) (pH 7.4) at 4°C, and then postfixed them for 48 hours with 4% paraformaldehyde and 0.2% picric acid in 0.1 mol/L PB at 4°C. The specimens were decalcified using K-CX (Falma, Tokyo, Japan) for 3 days, washed for 4 days with several changes of 0.1 mol/L PB containing 15% su-

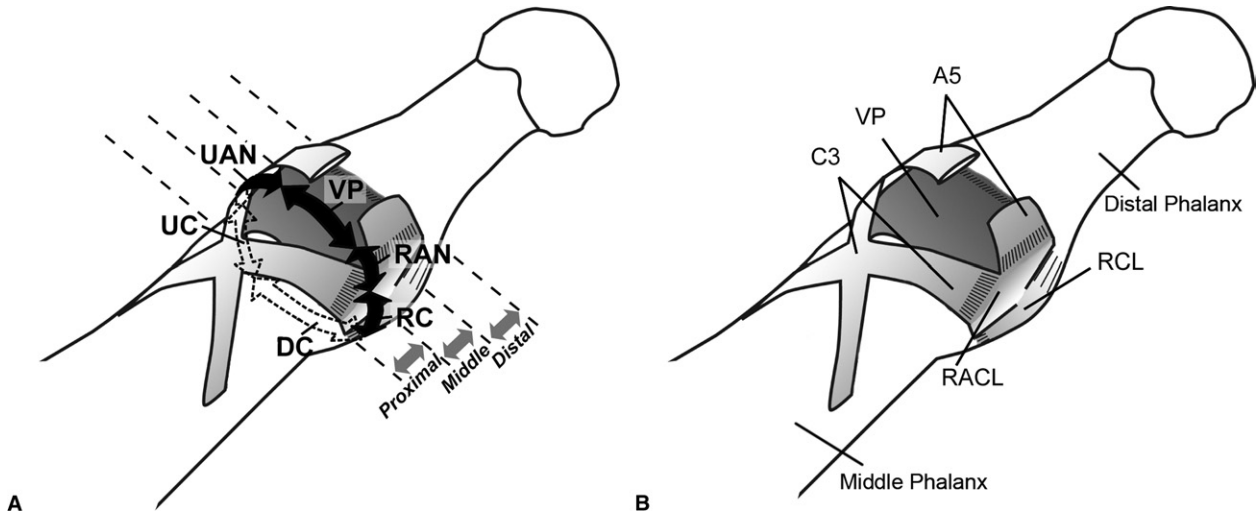

FIGURE 1: A Radial oblique view of the DIP joint. The DIP joint was divided into distal, middle, and proximal regions on the long axis. Each of the transverse sections was partitioned into DC, RC, UC, VP, RAN, and UAN, according to the anatomical soft tissue structures. **B** C3, Cruciate 3 pulley; A5, annular 5 pulley; RACL, radial accessory collateral ligament; RCL, radial collateral ligament.

crose, and then incubated overnight in 10% gelatin in 0.1 mol/L PB at 37°C. The gelatin-embedded specimens were cut transversely into 50-μm-thick sections in a cryostat and collected in 0.1 mol/L phosphate-buffered saline (PBS) at 4°C.

Serial mirror sections of the whole specimen were extracted at 500-μm intervals and then processed for immunohistochemistry and hematoxylin-eosin staining. For immunohistochemistry, sections were incubated for 2 days with an antibody against protein gene product 9.5 (PGP 9.5, rabbit polyclonal; Ultra Clone, Ltd., Wellow, UK) diluted 1:1,000 in 0.1 mol/L PBS (0.9% NaCl in 0.1 mol/L PB) containing 0.3% Triton X-100 (Nacalai Tesque, Kyoto, Japan) (PBST) at 4°C. To inactivate the endogenous peroxidase, the sections were treated with 0.1% H_2O_2 in 0.1 mol/L PBS followed with 0.1% phenylhydrazine in 0.1 mol/L PBS at room temperature (RT) for 30 minutes each. After washing for 30 minutes with PBST, the sections were incubated for 2 hours with biotinylated anti-rabbit immunoglobulin G (Vector Laboratories, Burlingame, CA) diluted 1:1,000 in PBST at RT. They were washed for 30 minutes with PBST and placed for 2 hours in avidin-biotin-peroxidase complex (ABC kit; Vector Laboratories) diluted 1:1,000 in PBST at RT. The immunoreaction was rendered visible by reaction with 0.05 mol/L Tris-HCl buffer (pH 7.6) containing 0.01% 3,3'-diaminobenzidine, 1% ammonium nickel sulfate, and 0.0003% H_2O_2 for 30 minutes at RT. Finally, the stained sections were dehydrated and mounted onto glass slides.

Silver staining method: Bodian method (type II nerve ending)

We fixed 6 DIP joints with 10% formalin and decalcified them with Plank-Rychlo solution (Wako, Osaka, Japan). The specimens were dehydrated with graded ethanol and embedded in paraffin according to standard histological procedures. The specimens were cut transversely into 20-μm-thick sections. Serial sections of the whole specimen were extracted at 500-μm intervals and immersed for 24 hours with 1% protein silver plus 4% copper solution at 37°C and for 10 minutes with 1% hydroquinone plus 5% neutral buffered formalin solution for reduction. The sections were then immersed for 5 minutes in 1% gold chloride solution and colored for 2 minutes with 1% oxalic acid solution. The stained sections were dehydrated and mounted onto glass slides.

Quantitative analysis

We divided serial transverse sections of the whole specimen extracted at 500-μm intervals into 3 regions along the longitudinal axis: distal, middle, and proximal (Fig. 1A). Each transverse section was partitioned into dorsal capsule (DC), radial capsule (RC), ulnar capsule (UC), volar plate (VP), radial assemblage nucleus (RAN), and ulnar assemblage nucleus (UAN), according to the anatomical soft tissue structures,[14,16,17] as shown in Figure 2A and B. The DC included the central slip of the extensor tendon, the RC included the radial collateral and accessory collateral ligament, and the UC included the ulnar collateral and accessory collateral ligament. Both the RAN and the UAN are located on the radial and ulnar side of the VP. To define areas of the RAN,

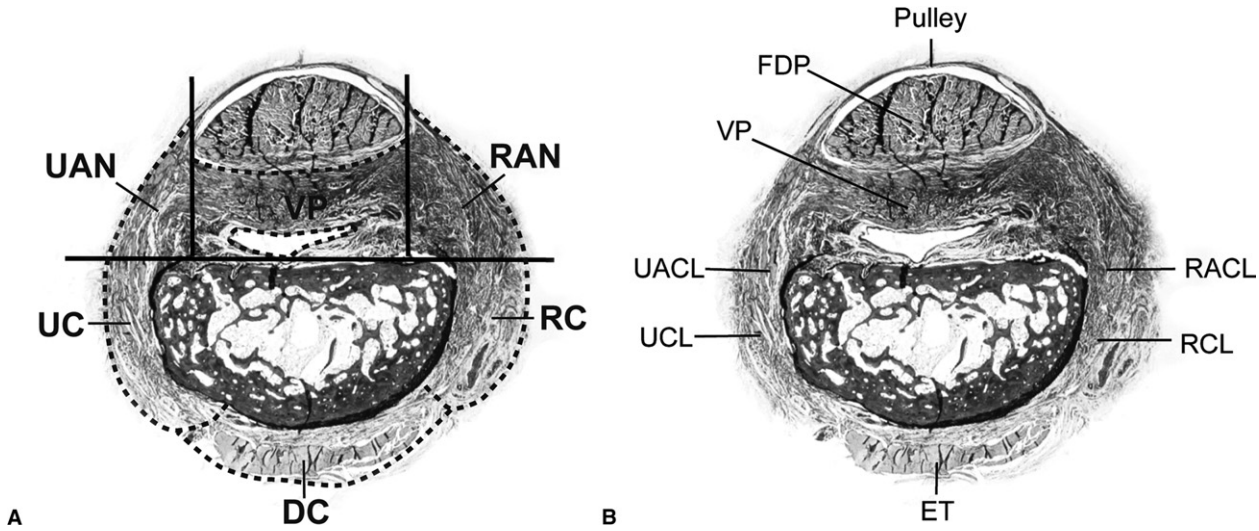

FIGURE 2: A Six regions of the transverse section at middle region. UAN, Ulnar assemblage nucleus. To define the regions of VP, UC, RC, RAN, and UAN, the 2 highest points of the volar side in the proximal and distal phalanx were joined by a line and 2 perpendicular lines were drawn from both the radial and the ulnar attachment of the pulley. The region of DC corresponded to the soft tissue structure. **B** Same section as **A**. FDP, Flexor digitorum profundus; RACL, radial accessory collateral ligament; RCL, radial collateral ligament; UACL, ulnar accessory collateral ligament; UCL, ulnar collateral ligament; ET, extensor tendon of the central slip.

UAN, VP, RC, and UC, the 2 highest points of the volar side in the proximal and distal phalanx were joined by a line. We then drew 2 perpendicular lines from both the radial and the ulnar attachment of the pulley. The region of DC corresponded to the central slip of the extensor tendon (Fig. 2A, B).

The C3 pulley contained the proximal region of the RAN and UAN, whereas the A5 pulley contained the middle and distal region. The accessory collateral ligament contained all the regions of the RAN and UAN (Fig. 1A, B).[14,16,17]

Light microscopic images of transverse sections were transferred to a monitor screen. All PGP 9.5-positive structures were type I nerve endings, but we observed no type III nerve endings. Therefore, the number of type I nerve endings in the 18 different regions (Figs. 1A, 2A) was counted and the corresponding areas were digitized and measured in hematoxylin-eosin–stained mirror sections using Image J software (National Institutes of Health, Bethesda, MD). We counted the number of silver-stained nerve endings (type II) in the 18 different regions and digitized and measured the corresponding areas in the same sections. Finally, the density of type I and type II nerve endings was calculated by dividing the total number of nerve endings by the total area measured in the 18 different regions.

Statistical analysis

Results are expressed as means ± SD. The densities of type I and type II nerve endings (number per square millimeter) were compared with 2-way analysis of variance (ANOVA) using SPSS v. 16.0J (SPSS Japan, Inc., Tokyo, Japan). We used 2-way ANOVA to evaluate the significance of differences in density of the type I and type II endings in the 18 regions: the first parameter was the proximal, middle, and distal regions of the DIP joint, and the second parameter was the 6 regions in the transverse sections. The results obtained by 2-way ANOVA showed that the interactions between values in the 3 (proximal, middle, and distal) regions on the long axis and those in the 6 regions in the transverse plane were significant ($p < .05$). Therefore, we performed one-way ANOVA and the post hoc Tukey test to compare the 18 different regions. Values of $p < .05$ were considered statistically significant.

RESULTS

According to the modified Freeman and Wyke classification,[5] type I and type II nerve endings were identified in the human DIP joint and surrounding structures, but no type III endings were identified in any region observed.

Our immunohistochemical technique successfully stained the PGP 9.5–positive nerve fibers in the DIP joint (Fig. 3A). We observed aggregation of nerve fibers (Fig. 3A, inset), identified by their size as type I nerve endings. In silver-stained sections, however, nerve fibers were difficult to detect, but characteristic lamellar formations of type II nerve endings, called

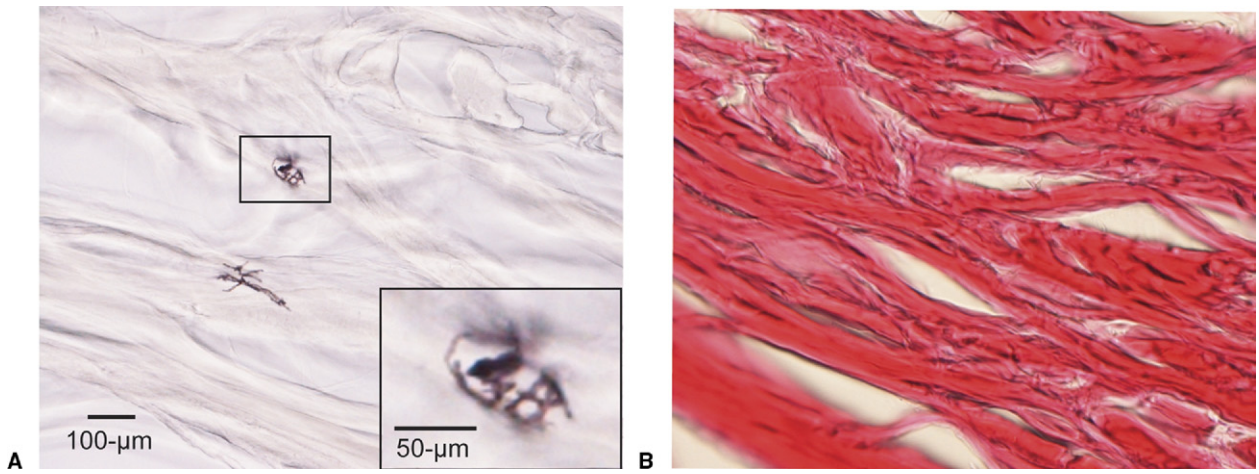

FIGURE 3: **A** PGP9.5-positive type I nerve endings were found in the VP. **A** Inset: higher magnification of the area enclosed by the rectangle in **A**. **B** Mirror section of **A** hematoxylin-eosin stain.

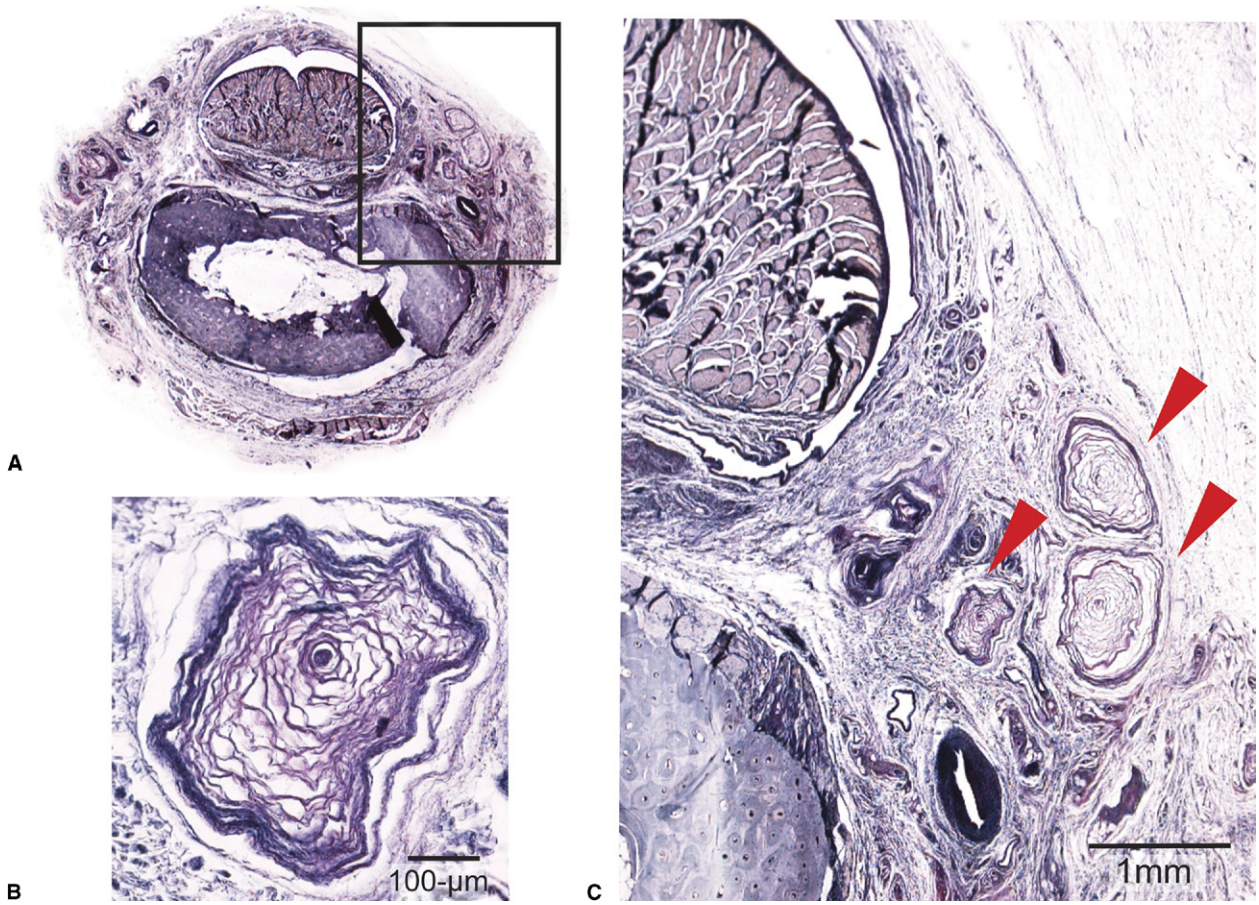

FIGURE 4: **A** Silver-stained section (magnification, ×5). **C** Inset of **A**: higher magnification of the area enclosed by the rectangle (RAN) in **A**. Aggregation of type II nerve endings in RAN. **B** Silver-stained type II ending. The characteristic lamellar formation is prominent.

Pacinian endings, were prominent (Fig. 4A, 4B, 4C [inset of A]). Such lamellar formations of type II nerve endings were difficult to observe with PGP 9.5 immunohistochemistry. Therefore, we used immunohistochemistry for PGP 9.5 to identify type I nerve endings, whereas we used silver staining to identify type II nerve endings.

TABLE 1. Density of Type I Nerve Endings

	RAN	VP	UAN	RC	UC	DC
Distal	0	1.9 ± 2.1	0	0	0	1.0 ± 1.4
Middle	0	0.1 ± 0.2	0	0	0	0
Proximal	0	0.4 ± 0.9	0	0	0	0

Data represent number per square millimeter.

Tables 1 and 2 respectively present the density of type I and type II nerve endings in the 18 different regions. Extensive analysis of multiple comparisons among different regions of the transverse sections showed that the density of type I nerve endings was not statistically significant (Fig. 5A). The density of type II nerve endings in the RAN in the proximal region was significantly higher than the density in the proximal region VP ($p < .001$), RC ($p < .001$), UC ($p < .001$), and DC ($p < .001$) (Fig. 5B). The density of type II nerve endings in the UAN in the proximal region was significantly higher than the density in the VP ($p = .004$), RC ($p < .001$), UC ($p < .001$), and DC ($p < .001$) in the proximal region (Fig. 5B). Comparison of the density of type II nerve endings among different regions of the DIP joints showed that the density in the RAN in the proximal region was significantly higher than that in the middle ($p < .001$) and distal ($p < .001$) regions of the DIP joints (Fi 5B). The density in the UAN in the proximal region was significantly higher than that in the middle ($p < .001$) and distal ($p < .001$) regions of the DIP joints (Fig. 5B).

DISCUSSION

We identified type I and II nerve endings in human DIP joints and surrounding structures and extensively examined their distributions. Results showed that type II nerve endings, called Pacini endings, were densely distributed in the RAN and UAN at the proximal region of the DIP joint and surrounding structures. Type I nerve endings, called Ruffini endings, were identified in VP and DC of the human DIP joint, but the density of type I nerve endings was not statistically significant.

Physiologically, type II nerve endings are known to be low-threshold, rapidly adapting receptors that respond to pressure and vibratory stimuli.[1] The type II nerve endings respond with one or 2 action potentials at the beginning and end of a pressure stimulus but are silent when the stimulus is constant in intensity.[19] In other words, the type II nerve endings are specialized in the detection of motion.[1] The type II nerve endings consist of concentrically arranged, fluid-filled outer lamellae of connective tissue that form a capsule surrounding the inner core consisting of nerve terminal.[1,19] When a stimulus first impinges on the type II nerve endings, the lamellae capsule is deformed, compressing the nerve terminal. During steady pressure, the outer lamellae of the capsule are compressed, absorbing the static load and preventing the deformation from being transmitted to the inner core and then to the nerve terminals.[19] When the pressure is removed, the lamellae capsule resumes its initial shape and the resultant tissue movement stimulates the nerve terminal again.[19]

In the present study, the type II nerve endings were notably distributed in both the proximal RAN and the UAN in the DIP joint and surrounding structures. The proximal RAN and UAN contained C3 pulley and radial and ulnar accessory collateral ligaments in the DIP joint.[14,16,17] In our previous study, distribution of type II nerve endings in PIP joints and surrounding structures showed similar results to the DIP joint and surrounding structures.[13] The type II nerve endings were substantially distributed in the proximal RAN and UAN, which contained C1 pulley and radial and ulnar accessory collateral ligaments in the PIP joint.[13]

In both PIP and DIP joints, the proximal RAN and UAN contained cruciate pulley and accessory collateral ligaments. In the human finger pulley system, it is well known that the A2, A3, and A4 pulleys in the finger are important in restraining bowstringing of the flexor tendons and facilitate smooth excursion of the tendon during finger flexion.[14,15,18] The cruciate pulley is not

TABLE 2. Density of Type II Nerve Endings

	RAN	VP	UAN	RC	UC	DC
Distal	0	0	0	0	0	0
Middle	2.1 ± 2.9	0.6 ± 1.1	3.3 ± 5.4	0	1.9 ± 0.4	0
Proximal	52.6 ± 27.5	7.3 ± 3.3	35.7 ± 11.2	0.7 ± 1.7	0	0

Data represent number per square millimeter.

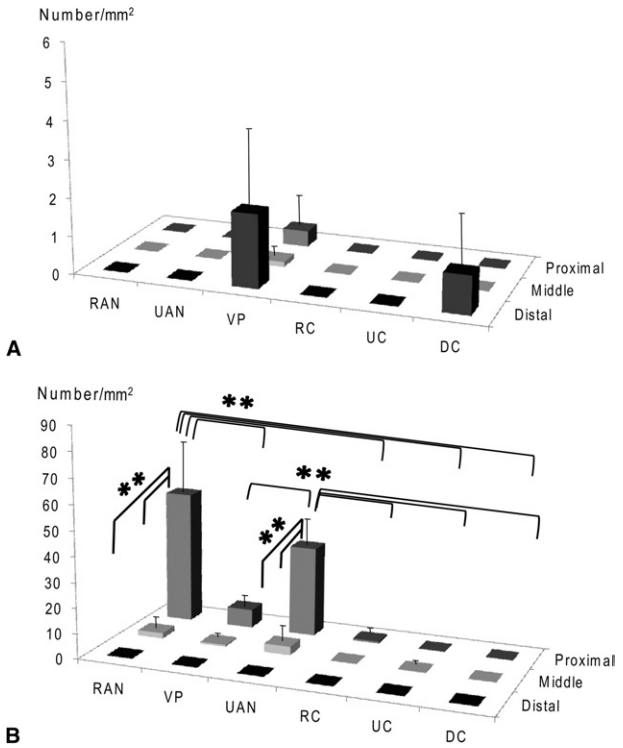

FIGURE 5: Comparison of the density of type I nerve endings **A** (n = 6) and the density of type II nerve endings **B** (n = 6). **p < .01.

believed to likely serve a major mechanical function.[15] Our results suggest that the C3 pulley and radial and ulnar accessory ligaments may act as a sensory generator that transmits a traction force to the radial and ulnar assemblage nuclei, because type II nerve endings are densely distributed in these regions. Our present and previous results might thus suggest an important function of the cruciate pulley in the finger pulley system.

Type I nerve endings are globular or ovoid and possess the characteristic feature of dense arborization of nerve fibers.[20] Physiologically, type I nerve endings are known to be low-threshold, slowly adapting receptors that sustain discharges in response to a constant stimulus; thus, they are considered to be stretch receptors.[1,7] The physiological function of the type I nerve ending might be understood via its morphological characteristics. Type I nerve endings are detected only at the dense collagen matrix of the articular capsule and are wound around bundles of collagen fibrils.[21] Therefore, type I nerve endings possibly sense the tension of the bundles of collagen fibrils.[21]

In this study, the age of our subjects was more than 70 years. Chang et al[22] reported that elderly subjects (age greater than 60 y) had a 40% to 42% reduction of epidermal nerves compared with young adults (19–39 y). Therefore, the number of nerve endings in the DIP joint and surrounding structures might be affected by aging.

In conclusion, we identified type I and type II nerve endings in the DIP joint and surrounding structures. The density of type II nerve endings was highest in both the RAN and the UAN in the proximal region of the DIP joint, suggesting that they might primarily sense mechanical stimuli from the C3 pulley and the accessory collateral ligament during finger movement.

REFERENCES

1. Kandel ER, Schwartz JH, Jessell TM, eds. Principles of neural science. 4th ed. New York: McGraw-Hill, 2000:430–450.
2. Tomita K, Berger EJ, Berger RA, Kraisarin J, An KN. Distribution of nerve endings in the human dorsal radiocarpal ligament. J Hand Surg 2007;32A:466–473.
3. McLain RF, Pickar JG. Mechanoreceptor endings in human thoracic and lumbar facet joints. Spine 1998;23:168–173.
4. Kennedy JC, Alexander IJ, Hayes KC. Nerve supply of the human knee and its functional importance. Am J Sports Med 1982;10:329–335.
5. O'Connor BL, Gonzales J. Mechanoreceptors of the medial collateral ligament of the cat knee joint. J Anat 1979;129:719–729.
6. Wyke B. The neurology of joints. Ann R Coll Surg Engl 1967;41: 25–50.
7. Boyd IA, Roberts TD. Proprioceptive discharges from stretch-receptors in the knee-joint of the cat. J Physiol 1953;122:38–58.
8. Clark FJ, Grigg P, Chapin JW. The contribution of articular receptors to proprioception with the fingers in humans. J Neurophysiol 1989; 61:186–193.
9. Edin BB. Finger joint movement sensitivity of non-cutaneous mechanoreceptor afferents in the human radial nerve. Exp Brain Res 1990;82:417–422.
10. Solomonow M, Baratta R, Zhou BH, Shoji H, Bose W, Beck C, et al. The synergistic action of the anterior cruciate ligament and thigh muscles in maintaining joint stability. Am J Sports Med 1987;15: 207–213.
11. Guanche C, Knatt T, Solomonow M, Lu Y, Baratta R. The synergistic action of the capsule and the shoulder muscles. Am J Sports Med 1995;23:301–306.
12. Phillips D, Petrie S, Solomonow M, Zhou BH, Guanche C, D'Ambrosia R. Ligamentomuscular protective reflex in the elbow. J Hand Surg 1997;22A:473–478.
13. Chikenji T, Suzuki D, Fujimiya M, Moriya T, Tsubota S. Distribution of nerve endings in the human proximal interphalangeal joint and surrounding structures. J Hand Surg 2010;35A:1286–1293.
14. Lin GT, Amadio PC, An KN, Cooney WP. Functional anatomy of the human digital flexor pulley system. J Hand Surg 1989;14A:949–956.
15. Doyle JR. Anatomy of the finger flexor tendon sheath and pulley system. J Hand Surg 1988;13A:473–484.
16. Zancolli E. Atlas of surgical anatomy of the hand. New York: Churchill Livingstone, 1992:149–151.
17. Craig SM. Anatomy of the joints of the fingers. Hand Clin 1992;8: 693–700.
18. Zhao CF, Amadio PC, Berglund L, An KN. The A3 pulley. J Hand Surg 2000;25A:270–276.
19. Kandel ER, Schwartz JH, Jessell TM, eds. Principles of neural science. 4th ed. New York: McGraw-Hill, 2000:411–429.
20. Freeman MA, Wyke B. The innervation of the knee joint. An anatomical and histological study in the cat. J Anat 1967;101:505–532.
21. Halata Z, Munger BL. The ultrastructure of Ruffini and Herbst corpuscles in the articular capsule of domestic pigeon. Anat Rec 1980;198:681–692.
22. Chang YC, Lin WM, Hsieh ST. Effects of aging on human skin innervation. Neuroreport 2004;15:149–153.